# Quantitative mapping of methionine sensitivity to oxidation in the copper-bound PcuC chaperone

Lionel Tarrago[a,b,1,*], Lise Molinelli[a,c], Maya Belghazi[d], Mathilde Tribout[b,2], David Lemaire[b], Pierre Legrand[e], Sandrine Grosse[b], David Pignol[b], Monique Sabaty[b], Thierry Tron[c], Pascal Arnoux[b,*]

From:

[a] Aix Marseille Univ, INRAE, BBF, Marseille, France

[b] Aix Marseille Univ, CEA, CNRS, BIAM, Saint Paul-Lez-Durance, France

[c] Aix Marseille Univ, CNRS, Centrale Marseille, ISM2, Marseille, France

[d] Aix Marseille Univ, CNRS, BIP, IMM, Marseille, France

[e] Synchrotron SOLEIL, L'Orme des Merisiers, F-91192, Gif-sur-Yvette, France

[1] Permanent address: Aix Marseille Univ, INRAE, BBF, Marseille, France

[2] Present address: Aix Marseille Univ, CNRS, LCB, IMM, Marseille, France

*Correspondence: Lionel Tarrago (lionel.tarrago@inrae.fr) or Pascal Arnoux (pascal.arnoux@cea.fr)

**Keywords:** cofactor biosynthesis, copper chaperone, metalloprotein, methionine oxidation, oxaziridine

**Abstract**

Copper is typically coordinated by histidine, cysteine, or methionine in proteins, and these residues are particularly sensitive to oxidation. However, it remains unclear whether copper-coordinating residues are more prone to oxidation than non-coordinating ones, and how their susceptibility changes between the apo and copper-bound states. The copper chaperone PcuC, important for cytochrome c oxidase assembly in bacteria, contains a canonical binding site composed of two histidines and two methionines ($H51x_nM63x_{22}H86xM88$), as well as a disordered C-terminal extension enriched in methionine and histidine. To quantify methionine oxidation sensitivity in both apo- and Cu-bound PcuC, we used a methionine-specific oxaziridine probe combined with mass spectrometry and compared labeling patterns to those generated by $^{18}O$-labeled hydrogen peroxide. We show that methionine residues display distinct oxidation sensitivities in the apoprotein, and that the oxaziridine reacts similarly to $H_2{}^{18}O_2$. Importantly, this probe enables quantification of methionine oxidation independently of hydroxyl radicals generated by copper-driven Fenton chemistry, which lacks residue specificity. In the copper-bound form, Cu binding strongly alters methionine reactivity, with a marked increase in oxidation of the coordinating Met63 and Met88. Structural analysis revealed that two copper ions occupy the canonical site, while the C-terminal extension does not contribute to coordination. Comparison of structural features and oxidation values showed that methionine sensitivity correlates with solvent exposure in the folded domain, but with local positive charge in the disordered region. These findings demonstrate that copper coordination modulates methionine oxidation, and that oxaziridine-based probes provide a powerful tool for mapping oxidation sensitivity in (metallo)proteins.

## 1. Introduction

Metals are essential in life, especially within proteins where they serve as critical cofactors for various biochemical reactions. Copper plays essential roles in biology as redox center in proteins involved in electron transfer, redox catalysis, and metal homeostasis [1]. Copper is commonly coordinated by histidine (His), cysteine (Cys), and methionine (Met) residues, with His and Cys predominantly found in redox-active sites while Met is mostly found in copper transporters and chaperone [2]. Copper can also bind proteins implicated in neurodegenerative diseases, such as α-synuclein and the prion protein [3,4]. The diversity of copper sites and ligands reflects the metal's versatility, but also the need for precise control to ensure correct metalation and prevent oxidative damage. Indeed, the copper-coordinating residues Cys, His, and Met are particularly sensitive to oxidation, leading to radical or oxygenated forms. Oxidants like hydrogen peroxide ($H_2O_2$) or hypochlorite have distinct reactivity towards amino acids, and the reaction of $H_2O_2$ with iron or copper in Fenton(-like) reaction generates strongly oxidant hydroxyl radicals [5,6]. While hypochlorite and hydroxyl radicals have broad reactivity and affect most amino acids and the protein backbone, $H_2O_2$ reacts specifically with Cys and Met [7]. In particular, Met can be oxidized into sulfoxide (MetO) and sulfone ($MetO_2$) [7,8]. Protein oxidation may have diverse consequences, from damage to regulated changes in function or activity. However, little is known about the sensitivity to oxidation of Cys, His, or Met within copper-binding proteins. It is not known whether these residues that are present in copper coordination sites, either in the apo- or copper-bound state, present a susceptibility to oxidation different from non-coordinating counterparts. Understanding the sensitivity of copper proteins to oxidation is crucial, as it can lead to their inactivation, as observed for superoxide dismutase and lytic polysaccharide monooxygenases [9–12]. It can also affect the structural properties of α-synuclein and the prion protein, with potential pathological outcomes [13,14]. In peptides mimicking copper-binding sites of the eukaryotic Ctr1 copper transporter, few evidence indicates that Cys is highly sensitive to oxidation contrary to Met or His [15,16]. Oxidation sensitivity of copper-binding Met in α-synuclein has also been observed, though quantitative data are lacking. In bacteria, such mechanisms remain poorly understood, despite their particular relevance for periplasmic proteins, which are exposed to copper-induced hydroxyl radical production and rely on

63 detoxification and export systems [5,17,18]. Consistently, it has been shown that the expression of the
64 methionine sulfoxide reductase (Msr) P/Q system, that repairs periplasmic protein by reducing oxidized Met
65 [19,20], is induced by the presence of an excess of copper in the periplasm through the activation of the
66 CusSR two-component system [21]. Bacterial membranes and mitochondria harbor the respiratory chain,
67 where cytochrome *c* oxidase (Cox) contains two copper atoms forming the CuA center within its periplasmic
68 catalytic subunit CoxB, which is essential for oxygen reduction [22]. Bacterial CoxB requires two
69 chaperones for its assembly: PrrC, homologous to eukaryotic Sco proteins, and PcuC, a cupredoxin-like
70 protein. This protein is often referred to as $PCu_AC$ but we use PcuC in this article to follow uniform
71 nomenclature of bacterial proteins. The sequence of events allowing Cu insertion in CoxB has been
72 evaluated in several bacterial species [23–26]. In the model proposed for *Cereibacter sphaeroides*, PcuC
73 acquires copper from the periplasm and transfers it to PrrC, which then assembles the $Cu_A$ center with one
74 Cu(I) and one Cu(II) [26]. Cu ions are sequentially transferred from one coordinating site to another [27,28].
75 Particularly, CoxB coordinates the two Cu with two Cys, two His, one Met and one Glu in a
76 $Hx_{34}CxExCx_3Hx_2M$ motif [24,29]. PrrC uses two Cys and one His in the $Cx_3Cx_nH$ motif to coordinate a
77 Cu(II) ion [24]. It has been shown that copper-coordinating Cys of both CoxB and PrrC can form disulfide
78 bonds that need to be reduced by the dedicated thiol-reductase TplA before copper insertion [30]. PcuC is
79 widely conserved among bacteria and most homologs possess a Cu(I)-binding motif composed of two Met
80 and two His ($Hx_nMx_{22}HxM$) and have an additional C-terminal extension rich in Met and His, proposed to
81 bind a second copper ion [23,24,31]. Other types lack this extension or bind copper in a His-brace [24,32].
82 The *C. sphaeroides* PcuC is a representative model for studying copper's role in protein oxidation.

83 In this work, we evaluated the sensitivity of PcuC's Met to oxidation, either in the apo or in the copper-
84 loaded protein by using two molecules reacting with Met: i) $^{18}O$-labeled hydrogen peroxide, and ii) an
85 oxaziridine probe (**Fig. 1A**). We quantified the level of oxidation of each Met by trypsin proteolysis and
86 liquid chromatography coupled with tandem mass spectrometry (LC-MS/MS). $H_2O_2$ is a natural oxidant
87 potentially encountered by bacteria. In the absence of Cys, as it is the case for PcuC, it allows the specific

88 oxidation of Met [7,20]. The use of $^{18}O$-labeling avoid the quantification of artifactual Met oxidation
89 potentially arising in proteomic analysis [33–35]. However, $H_2O_2$ can react with the metal in the copper-
90 loaded protein, generating highly reactive hydroxyl radicals that may oxidize peptide bonds and residues
91 other than Met. To specifically quantify methionine sensitivity to oxidation in the copper-loaded protein
92 independently of Fenton reaction, we used an oxaziridine probe designed for selective reactivity with Met
93 [36,37]. This probe operates via nitrogen atom transfer, where the electrophilic nitrogen of the strained N–
94 O bond reacts with the thioether sulfur, forming a stable sulfimide adduct (**Fig. 1B**). We first assessed Met
95 sensitivity in the apo form using $H_2{}^{18}O_2$ and then with the oxaziridine probe, allowing comparison of both
96 approaches. Then, we applied the probe to the copper-loaded protein to evaluate the impact of Cu
97 coordination on Met oxidation. Finally, we determined the three-dimensional structures of both apo and
98 copper-bound PcuC and integrated these structural insights with oxidation data to identify determinants of
99 Met susceptibility to oxidation.

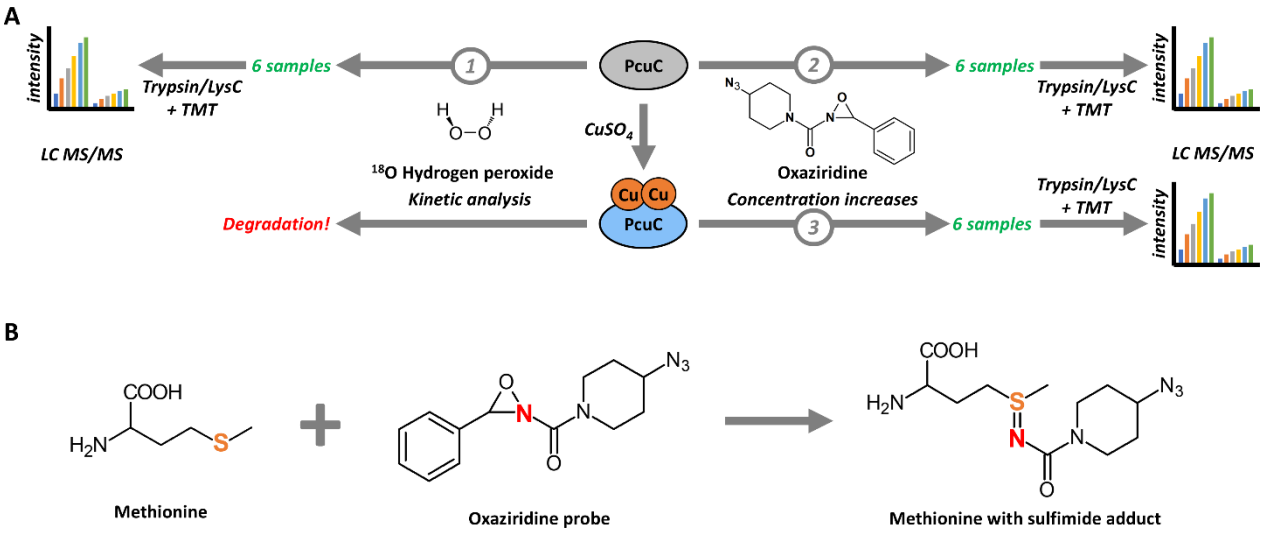


**Fig. 1. Utilization of an oxaziridine probe to quantify Met sensitivity to oxidation in PcuC and comparison with $H_2{}^{18}O_2$. (A)** Experimental design. Apo-PcuC was oxidized with $H_2{}^{18}O_2$ in kinetic experiment (*1*) and apo-PcuC (*2*) or copper-bound PcuC (*3*) was incubated with increasing concentrations of oxaziridine probe. For these three analyses, six samples, prepared in triplicates, were digested with Trypsin/Lys C mix and analyzed simultaneously by LC-MS/MS using tandem mass tags (TMT) labeling. Analysis of Cu-loaded PcuC with $H_2{}^{18}O_2$ was not performed because of protein degradation (*see* **Fig. S4B**). **(B)** The oxaziridine probe ((4-azidopiperidin-1-yl)(3-phenyl-1,2-oxaziridin-2-yl)methanone) oxidizes the sulfur atom in Met, resulting in a nitrogen transfer reaction. The sulfur of Met is covalently linked to the nitrogen atom of the oxaziridine probe via a sulfimide bond.

## 2. Results and Discussion

### 2.1. Methionine residues of the PcuC apoprotein have various sensitivity to oxidation

The copper chaperone PcuC contains eight Met residues: one isolated in the first half of the primary sequence (Met25), two pairs clustered together (Met61 and Met63, and Met88 and Met90), and three near the C-terminus (Met128, Met132, and Met135) (**Fig. 2A**). Using the purified recombinant apo-PcuC we first confirmed that it contains oxidizable Met residues and thus is relevant to quantify susceptibility to Met oxidation. It has up to seven MetO formed simultaneously by oxidation with $H_2O_2$ and most of which are reducible by the methionine sulfoxide reductase MsrP (**Supplemental Results 2.1, Fig. S1**). To quantify the sensitivity of the Met residues in the apo-PcuC individually, we incubated the protein with 1,000 molar equivalents of $H_2{}^{18}O_2$ for 2 to 60 minutes and oxidized residue were quantified (**Fig. 2B, S2B**). An SDS-PAGE analysis of the samples revealed a delay in protein migration, as observed for non-isotopic $H_2O_2$, confirming that oxidation occurred (**Fig. S2A**). The identification and quantification of $^{18}$O-Met revealed that the most abundant form was $^{18}$O-sulfoxide, with only traces of $^{18}$O-containing sulfone detected (**Fig. S2B**). The search for oxidized form of His (oxoHis) revealed only extremely low levels, confirming that Met residues were the target of oxidation by $H_2{}^{18}O_2$ (**Fig. S2C**). The analysis of the kinetics of oxidation revealed striking differences in the reactivity of the Met residues (**Fig. 2B, E**). Indeed, Met25 remained reduced throughout the treatment while Met135 was rapidly and extensively oxidized, up to ~93% after 60 minutes. Met63, which is part of the copper-coordinating site, was the second most oxidized residue, reaching ~45% by the end of the kinetics. The other Met residues showed intermediate levels of oxidation, all remaining below 50%. Interestingly, the oxidation kinetics of Met132 displayed a unique pattern compared to the other reactive Met residues. While for the other residues oxidation level quickly reached a plateau or increased linearly (Met61, Met128), Met132 oxidation level remained low at early timepoints but eventually increased to ~42%, like the level observed for Met63 (**Fig. 2B**). This behavior suggests that Met132 may be a secondary target for oxidation, becoming oxidized only after the more sensitive residues, Met63, Met90, and Met135. Based on final oxidation levels, Met reactivity in apo-PcuC ranked from least to most oxidized: Met25, Met128, Met88, Met61, Met90, Met132, Met63, Met135.

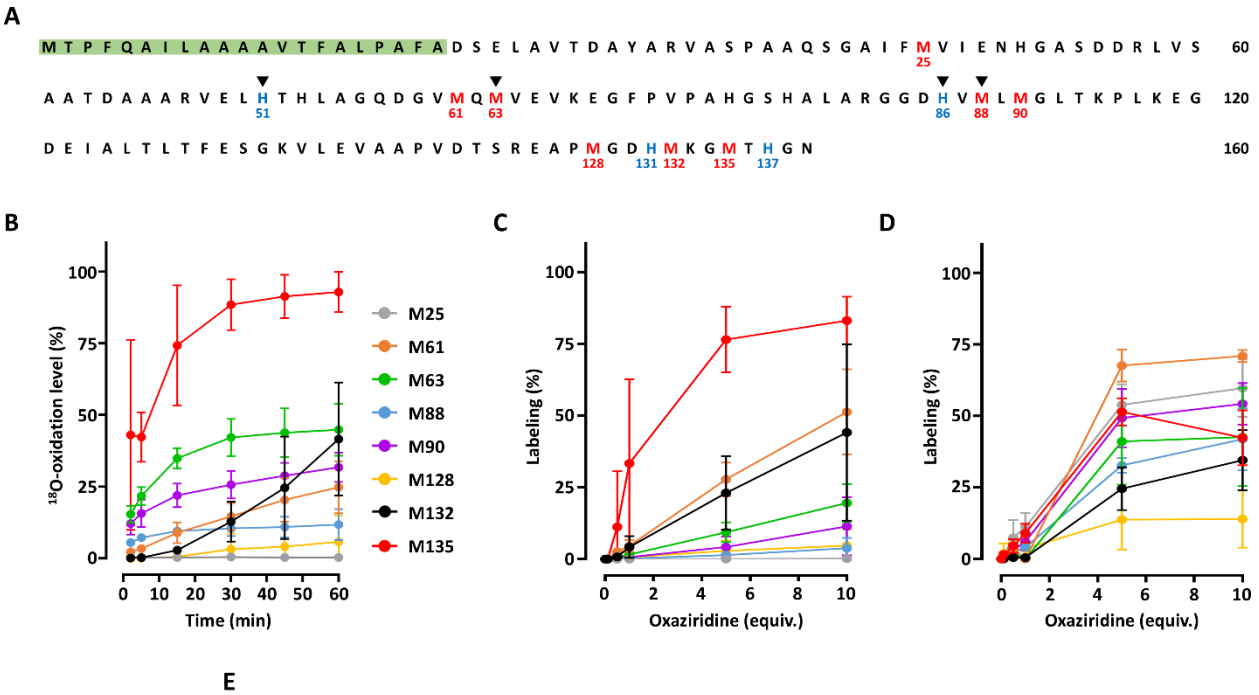


E

| | M25 | M61 | M63 | M88 | M90 | M128 | M132 | M135 |
|---|---|---|---|---|---|---|---|---|
| PcuC + $H_2{}^{18}O_2$ | 0 | 25 | 45 | 12 | 32 | 6 | 42 | 93 |
| PcuC + oxaziridine | 0 | 51 | 20 | 4 | 11 | 5 | 44 | 83 |
| Cu-PcuC + oxaridine | 35 | 71 | 43 | 42 | 54 | 14 | 60 | 42 |

**Fig. 2. Quantification of Met sensitivity to oxidation in apo- and Cu-loaded PcuC using $H_2{}^{18}O_2$ and an oxaziridine probe. (A)** Amino acid sequence of PcuC in single letter. The eight Met residues are shown in *red* with numbering below, amino acids on *green* background correspond to the periplasmic peptide signal and *black* triangles indicate Cu-coordinating residues. Met are numbered considering Asp as first residue after removal of the peptide signal. **(B)** Time-resolved percentage of oxidation of the eight Met residues of the apo-PcuC after incubation with $H_2{}^{18}O_2$. Apo-PcuC was incubated with 1,000 molar equivalents (equiv.) of $H_2{}^{18}O_2$ for 2, 5, 15, 30, 45 and 60 min and the reaction stopped with catalase. Percentages were calculated by summing the relative intensities of all Met forms, grouping $^{18}O$-containing species as oxidized and others as non-oxidized. **(C)** Percentage of labeling of the apo-PcuC after incubation with the oxaziridine probe. Apo-PcuC was incubated with 0, 0.1, 0.5, 1, 5 or 10 equiv. of the oxaziridine probe and the reaction stopped by desalting. **(D)** Percentage of labeling of the Cu-loaded PcuC after incubation with the oxaziridine probe. Cu-loaded PcuC was incubated with the oxaziridine probe similarly to the apoprotein. Note that for Met135, the lower mean value at 10 versus 5 equivalents falls within the experimental standard deviation. **(E)** Heatmap showing the final percentage of oxidation or labeling of the eight Met residues of PcuC, using a *blue*-to-*red* color scale, with *blue* and *red* representing the lowest and highest values of modification, respectively. Underlined Met63 and Met88 belong to the Cu-binding site.

154 **2.2. The oxaziridine probe reactivity toward Met is similar to that of hydrogen peroxide**

155 With the aim of quantifying Met sensitivity in the copper-loaded PcuC, we used an oxaziridine probe
156 [36,37]. First, we validated its ability to bind the apo-PcuC and its potential usability to quantify the
157 sensitivity of PcuC's Met residues to oxidation (**Supplemental Results 2.2, Fig. S3**). Our first approach
158 was to determine whether it can report similar results to those obtained using $H_2{}^{18}O_2$ with apo-PcuC. To do
159 so, we designed a slightly different strategy as chemical probes are usually used at several concentrations
160 to identify reactive residues in activity-based protein profiling or related approaches [36,38]. Thus, we
161 incubated the apo-PcuC with 0 to 10 molar equivalents of probe and quantified the labeling of each Met
162 after trypsin proteolysis and LC-MS/MS (**Fig. 2C, E**). The overall pattern closely matched the one obtained
163 with $H_2{}^{18}O_2$: Met25 was unlabeled, while Met135 was the most reactive, reaching ~83% with 10 equivalents
164 of probe. Both Met88 and Met128 were found labeled around 5%. Similarly, Met132 labeling percentage
165 (~44%) was nearly identical to the values obtained with $H_2{}^{18}O_2$. Met88 and Met128 showed low labeling
166 (~5%), and Met132 reached ~44%, consistent with $H_2{}^{18}O_2$ results. Differences were observed for Met63
167 and Met90, that were less labeled (~20% and ~11%, respectively), whereas Met61 showed higher labeling
168 (~51%). At the highest probe concentration, the reactivity ranking of Met residues in apo-PcuC was: Met25,
169 Met88, Met128, Met90, Met63, Met132, Met61, Met135. Consistently with the results obtained with
170 $H_2{}^{18}O_2$, this shows that copper-coordinating Met63 and Met88 do not present a sensitivity to oxidation
171 particularly different from that of the other residues. These results indicated that the use of the oxaziridine
172 probe is relevant to quantify Met sensitivity to oxidation in copper-loaded PcuC. To our knowledge,
173 although it was previously used to identify oxidizable Met residues [36,39], the reactivity of the oxaziridine
174 probes was never compared to physiological oxidants. This showed that the oxaziridine probe effectively
175 mimics $H_2O_2$-induced oxidation and is very likely relevant to identify redox-active Met residues in proteins
176 from various biological contexts.

177

178 **2.3. Cu binding strongly alters PcuC's Met sensitivity to oxidation**

179 We then sought to evaluate whether the presence of copper in PcuC affects Met sensitivity to oxidation
180 using the same approach. First, we incubated the protein with increasing concentration of $CuSO_4$ and
181 observed that two coppers could be bound to the protein using non-denaturing ESI-MS (**Fig. S4A**), as shown
182 for the *B. diazoefficiens* homolog [24]. As anticipated, the incubation of the copper-loaded PcuC with 1,000
183 equivalents of $H_2{}^{18}O_2$ resulted in a quick and complete protein degradation (**Fig. S4B**). This was very likely
184 due to Fenton-like reaction occurring between the peroxide and the copper, either bound to the protein or
185 free in the solution because of remaining trace despite the desalting. Using the probe on the copper-loaded
186 PcuC revealed a very different profile than for the apo protein (**Fig. 2D, E**). Indeed, we first noticed that all
187 Met residues were labeled, including Met25. By comparison with the apo-PcuC, we observed strong
188 increases for Met25, Met63, Met88 and Met90 labeling. The most labeled became Met61, followed by
189 Met132, while the level of labeling of Met135 strongly decreased. Interestingly, the reactivity of the copper-
190 ligand Met63 and Met88 increased by 2.1-fold and 3.5-fold, respectively (**Fig. 2D, E**). This indicates that
191 copper-binding increases Met sensitivity to oxidation. At the highest probe concentration, the reactivity
192 ranking in Cu-loaded PcuC was: Met128, Met25, Met88, Met135, Met63, Met90, Met132, and Met61. The
193 change in reactivity of the copper-coordinating Met63 and Met88 could be attributed to alterations in the
194 electronic density on sulfur atoms, as copper coordination withdraws electron density, increasing the
195 electrophilicity of sulfur. Additionally, copper binding might stabilize the Met lateral chain in a
196 conformation that favors oxidation. The increased sensitivity of the other Met not directly coordinating
197 copper, may result from the initial oxidation of the coordinating Met63 and Met88, which could alter the
198 protein's folding, thereby enhancing the overall accessibility and reactivity of other Met residues. Such
199 initial oxidation events has been shown to increase protein hydrophobicity and potentially favor further
200 oxidation [40,41]. The apparent decrease in the sensitivity of Met135 is most likely due to the increase in
201 sensitivity of the other Met residues, as it is unlikely that the structural properties have been modified for
202 this Met (the C-terminal part remained unfolded, *vide infra*).

203 **2.4. PcuC coordinates two Cu ions at the canonical Cu binding site**

204 To evaluate whether structural determinants can explain the observed differences of Met residues
205 reactivity, we solved the tridimensional structures of the apo and copper-bound PcuC by X-ray
206 crystallography (**Fig. 3**). The structure of the apo-PcuC was solved at 1.05 Å resolution in a $P4_32_12$ space
207 group obtained from a crystal grown in sodium citrate at pH 8.5 (**Table S1**). The structure is typical for
208 homologs of this protein family, i.e. a seven stranded β-barrel with one side of this barrel containing three
209 additional strands, which include the conserved Met and His residues involved in copper binding. Two parts
210 of the protein could not be resolved: the first spans residues Ala55 to Met61, while the second corresponds
211 to the C-terminus from Arg124 and includes Met128, Met132 and Met135 (**Fig. 3A**). These parts are very
212 likely flexible in the protein, and the C-terminal part was predicted to be disordered (**Fig. S5**). To obtain
213 experimental data on copper binding to PcuC, we added ten copper equivalents to the protein and re-
214 screened for crystallization. We obtained crystals that clearly showed two sites of high electron density,
215 very likely corresponding to metals, but they were affected by translational non-crystallographic symmetry
216 (**Supplemental Results 2.4**). Then, by mixing the copper-loaded PcuC with 20% PEG 6000, 1 M LiCl2 and
217 0.1 M citric acid at pH 4.0 in a second crystallization attempt, we obtained crystals that diffracted to 2.75 Å
218 resolution and the elucidated structure showed the presence of two copper ions (**Table S1, Fig. 3B**). One
219 copper (Cu1) is bound to Met88 Sδ (2.6 Å) and His86 Nδ (2.1 Å), similarly to what is observed in the PcuC
220 homologs from *Streptomyces lividans* [42] and *Thermus thermophilus* [23]. However, in these homologs
221 the copper is coordinated by two other ligands (corresponding to His51 and Met63), whereas in the structure
222 of *C. sphaeroides* PcuC a water molecule linked the copper to Nδ of His51 (2.7 Å; Cu1-HOH = 3 Å), and
223 Met63 adopted such a conformation that its side chain was not in the coordination sphere of Cu1 (the
224 distance Cu1 to Met63 Sδ is 5.5Å). Finally, what we interpreted as a citrate molecule, very likely coming
225 from the crystallization media, participated in the coordination sphere of this copper with a bidentate
226 interaction from one carboxylate moiety (Cu1-OA1 = 2.4 Å and Cu1-OA2 = 2.9Å). Overall, although the
227 position of this copper binding site is conserved between the three homologs structurally characterized, the

228 coordination sphere is different in *C. sphaeroides* PcuC. The additional copper ion (Cu2) observed in the
229 structure of *C. sphaeroides* PcuC was bound by Nε of His53 (1.8 Å) and three oxygen atoms from the three
230 carboxylate moieties of citric acid (2.7 Å, 3.1Å and 3.1 Å; **Fig. 3B**). Altogether, these results show that
231 PcuC could bind two coppers without the involvement of the unfolded C-terminal part. This finding was
232 unexpected given the results obtained for the *B. diazoefficiens* PcuC homolog [24]. While it is possible that
233 the two chaperones function differently, several elements support a unified model that reconciles both sets
234 of results. In this model, a first copper ion is stably coordinated in the canonical site (high-affinity), while a
235 second copper ion oscillates between various positions along the C-terminal extension and the coordination
236 site observed in our structure (low-affinity) (**Supplemental Discussion**).

237

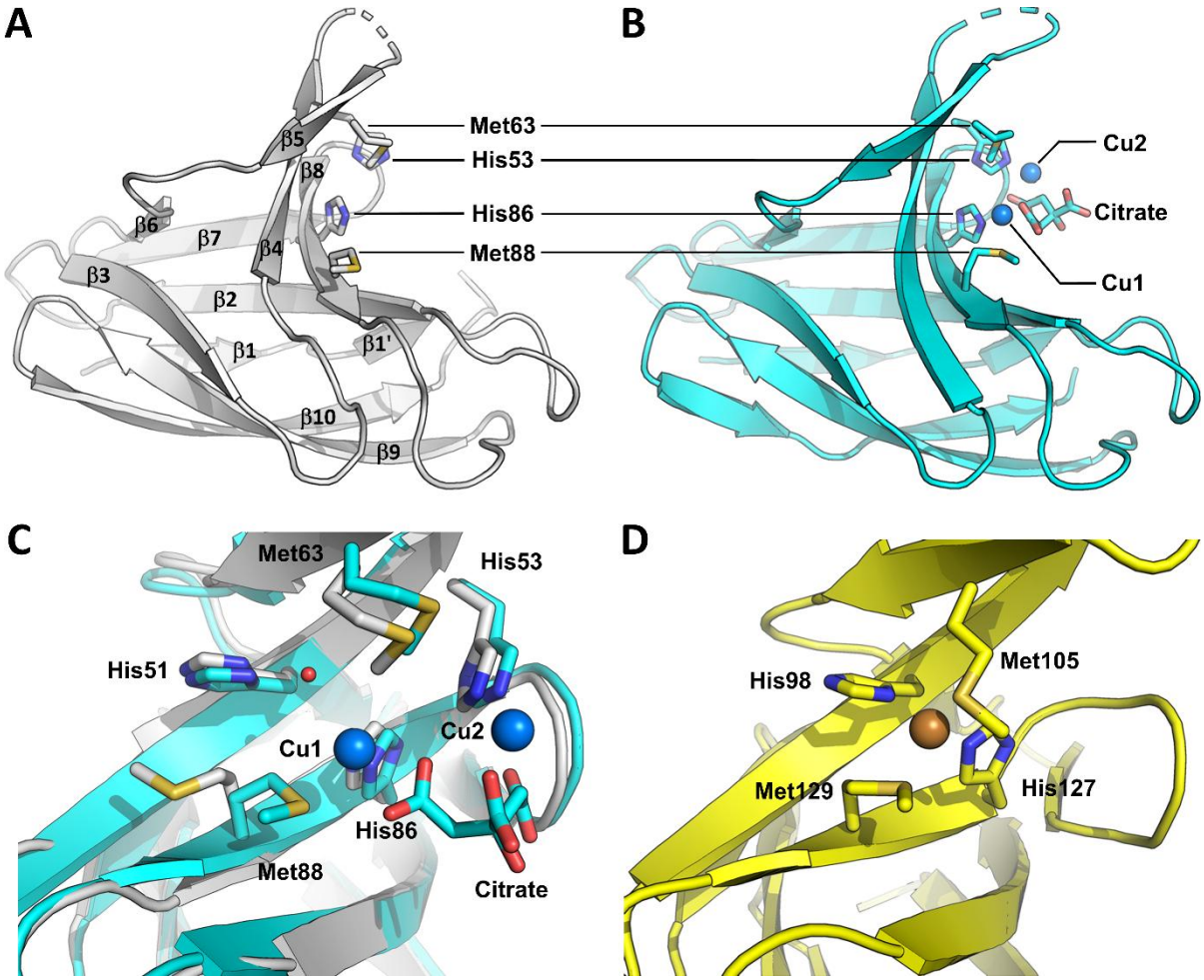


**Fig. 3. Structural characterization of apo-PcuC and Cu-loaded PcuC.** Overall structure of the apo form of PcuC (PDB 9REZ) **(A)** and the Cu-loaded form of PcuC (PDB 9RF0) **(B)**. **(C)** Superimposition of both the apo-and copper-bound form of PcuC with the side chains of the discussed residues shown in stick. **(D)** Details of the Cu-binding site of *S. lividans* PcuC (PDB 3ZJA).

243 **2.5. Met oxidation sensitivity correlates with solvent exposure in the folded region but with**
244 **positive charge in the unfolded C-terminal extension**

245 To understand the factors influencing Met oxidation in PcuC, we analyzed the solvent exposure and local
246 charges surrounding each Met in both apo- and Cu-bound structures. As the unfolded C-terminal extension
247 containing Met128, Met132, and Met135 was unresolved, we used an AlphaFold model to complete the
248 analysis (**Supplemental Results 2.5, Fig. S6A**). In the folded region (encompassing Met25 to Met90),
249 solvent exposure values were consistent between the resolved and modeled structures. Met25 showed
250 minimal exposure, while Met61 and Met63 were among the most exposed. Met128, Met132, and Met135,
251 in the unfolded C-terminal extension, displayed high solvent exposure in the model (**Fig. 4A**). We assumed
252 that the C-terminal extension remains unstructured in both the apo- and Cu-PcuC, and the exposure values
253 for these Met residues are similar to the model. To determine whether oxidation sensitivity correlates with
254 solvent exposure, we plotted the values of oxidation determined with $^{18}$O-labeled hydrogen peroxide and
255 oxaziridine as function of the Met exposure values for both the apo- and the copper-loaded PcuC structures
256 (**Fig. 4C, D**). In apo-PcuC, oxidation levels correlated positively with solvent exposure for Met residues in
257 the folded region ($R^2$ = 0.48 for $H_2{}^{18}O_2$ and $R^2$ = 0.90 for oxaziridine). A similar positive correlation was
258 observed using the solvent exposure values from the AlphaFold model (**Fig. S6B**). Surprisingly, the C-
259 terminal Met residues showed a strong negative correlation between oxidation and solvent exposure ($R^2$ =
260 0.99). Similar trends were observed in Cu-loaded PcuC, though with lower correlation values (**Fig. 4C**).
261 Strikingly, the most exposed Met128 was among the least oxidized, both with $H_2{}^{18}O_2$ and the oxaziridine
262 probe, and regardless of copper presence. To explain this discrepancy in the disordered region, we
263 considered the electrostatic environment. Surface charge maps revealed that, while most of the protein
264 surface is neutral or negatively charged, the C-terminal region includes a localized positive charge due to a
265 lysine (**Fig. S7A, B, C**). We quantified the partial charge within 5.5 Å of each Met sulfur (**Fig. 4D**). In the
266 folded domain, no correlation was found between oxidation and local charge (**Fig. S7D, E**). However, for
267 the C-terminal Met residues, we observed a strong positive correlation between oxidation sensitivity and
268 positive local charge ($R^2$ = 0.92–0.97 in apo-PcuC) (**Fig. 4E**). These results indicated that the oxidation

sensitivity of the Met residues belonging to the unfolded C-terminal part of PcuC was positively correlated with the positive partial charge surrounding the sulfur atom of the Met. Together, these results reveal that distinct factors govern metal oxidation in different structural contexts of PcuC: solvent exposure is crucial in the folded part, while local positive charge controls reactivity in the unfolded part. These results are consistent with the fact that solvent exposure plays very likely a major role in Met sensitivity to oxidation, as shown previously [43–45], but that other factors should be considered [46,47]. This suggests that Met sensitivity to oxidation might be protein and Met dependent and should be determined for each protein of interest.

**A**

| | M25 | M61 | M63 | M88 | M90 | M128 | M132 | M135 |
|---|---|---|---|---|---|---|---|---|
| PcuC (AF) | 3 | 107 | 116 | 27 | 80 | 184 | 169 | 148 |
| Apo-PcuC | 3 | 153 | 106 | 29 | 63 | *n.d.* | *n.d.* | *n.d.* |
| Cu-PcuC | 3 | 99 | 92 | 35 | 38 | *n.d.* | *n.d.* | *n.d.* |

**D**

| | M25 | M61 | M63 | M88 | M90 | M128 | M132 | M135 |
|---|---|---|---|---|---|---|---|---|
| PcuC (AF) | -0.493 | 0.944 | -0.006 | -0.986 | 1.716 | 0.023 | 0.287 | 0.420 |
| Apo-PcuC | -0.152 | -0.832 | -0.666 | -0.447 | 0.998 | *n.d.* | *n.d.* | *n.d.* |
| Cu-PcuC | -1.22 | -1.61 | 0.193 | 0.982 | -1.1 | *n.d.* | *n.d.* | *n.d.* |

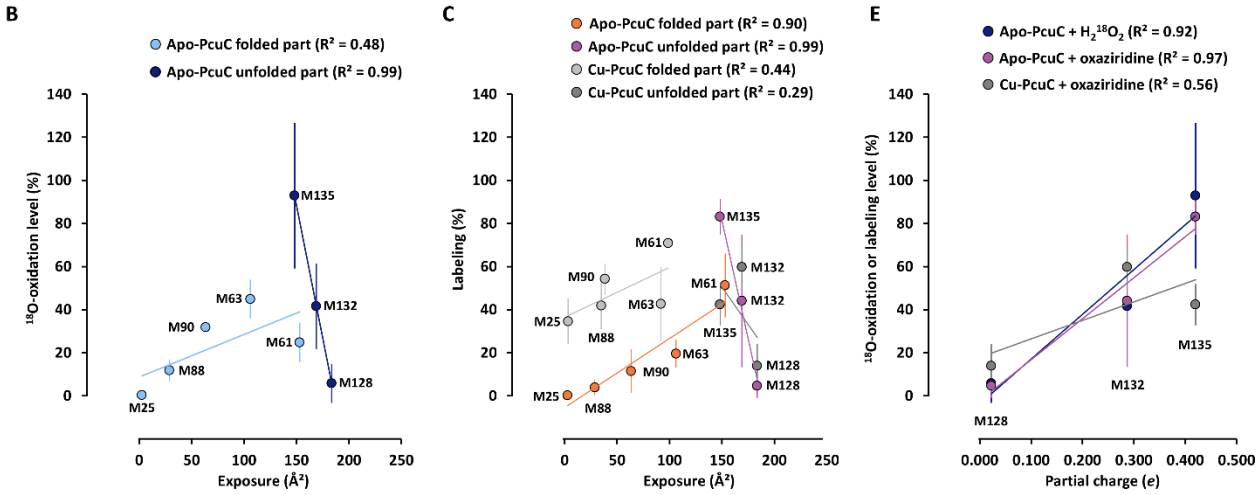


**Fig. 4. Correlation of Met oxidation sensitivity with solvent exposure and local charge. (A)** Heatmap showing the solvent exposure (Å²) of the Met, using a *blue*-to-*red* color scale, with *blue* and *red* representing the lowest and highest exposure, respectively. *n.d., not determined.* Underlined Met63 and Met88 belong to the Cu-binding site. **(B)** Plot of oxidation level of the Met residues as function of solvent exposure for the apo-PcuC after 60 min oxidation with $H_2{}^{18}O_2$ with independent linear regressions for the Met residues of the folded part and the unfolded C-terminal part. **(C)** Plot of oxidation level of the Met residues as function of solvent exposure for the apo- and Cu-loaded PcuC after exposure to 10 equivalents of oxaziridine with independent linear regressions for the Met residues of the folded part and the unfolded C-terminal part. **(D)** Heatmap showing the partial charge of the environment surrounding the sulfur of the Met, using a *blue*-to-*red* color scale, with *blue* and *red* representing the more negative and positive charge, respectively. *n.r., not resolved.* Underlined Met63 and Met88 belong to the canonical Cu-binding site. **(E)** Plot of oxidation of the Met residues from the C-terminal unfolded part determined with $H_2{}^{18}O_2$ and oxaziridine as function of the partial charge of the environment surrounding the sulfur of the Met determined on the AlphaFold model for the apo- and Cu-loaded PcuC with linear regressions.

293 **3. Conclusion**

294 In this study, we showed that the recently developed oxaziridine probe reacts with Met residues similarly
295 to $H_2{}^{18}O_2$, using the copper chaperone PcuC from *C. sphaeroides* as a model. This suggests the probe is a
296 reliable tool for quantitatively mapping Met oxidation sensitivity in any protein, including in
297 metalloproteins. Copper-coordinating Met residues are not significantly more or less sensitive to oxidation
298 than non-coordinating ones. We also provide new insights into the function of the conserved, disordered C-
299 terminal extension present in most PcuC homologs. This region could play a dual role: facilitating copper
300 incorporation into the coordination site, as suggested for copper transporters and oxidases [17,48], and
301 protecting against oxidative stress via Met135, a highly oxidation-sensitive residue. Met135 may act as a
302 local scavenger of reactive species and be regenerated by the periplasmic reductase MsrP, ensuring efficient
303 copper delivery and CoxB assembly, ultimately supporting proper bacterial respiration.

304

305 **4. Methods**

306 **4.1. Protein and chemicals**

307 PcuC was produced and purified as described [49]. $^{18}O$-labeled hydrogen peroxide and dibenzocyclooctyne-
308 Cyanine5 fluorophore (DBCO-Cy5) were purchased from Sigma-Aldrich. Initial concentration of
309 commercial $H_2{}^{18}O_2$ was estimated to be ~450 mM using FOX method [50]. The oxaziridine probe ((4-
310 azidopiperidin-1-yl)(3-phenyl-1,2-oxaziridin-2-yl)methanone) was synthetized according to [37] and
311 validated by NMR (**Fig. S8**). Protein concentrations were determined using the Bradford method (Bio-Rad
312 Protein Assay Dye Reagent Concentrate). SDS-PAGE were performed using Bolt™ pre-cast gel system
313 (ThermoFisher) using 12% polyacrylamide gels and 2-(N-Morpholino)ethanesulfonic acid (MES) running
314 buffer. Visible and fluorescent imaging were performed using Amersham ImageQuant™ 800 (Cytiva).

315 **4.2. PcuC oxidation, Cu-loading and labeling with the oxaziridine probe**

316 Apo-PcuC (70 µM) was oxidized with 10, 100, 500 or 1,000 molar equivalents (equiv.) of $H_2O_2$ in 50 mM
317 3-(N-Morpholino)propanesulfonic acid (MOPS) buffer at pH 8.0 for 1 h and the reaction was stopped by
318 adding excess dithiothreitol (DTT) (100 mM) and subsequent desalting using Sephadex G-10 (PD MidiTrap
319 G-10, Cytiva). For oxidation with $H_2{}^{18}O_2$, PcuC (100 µM), apo or Cu-loaded, was incubated for 2, 5, 15,
320 30, 45 and 60 min with 1,000 equiv. of $H_2{}^{18}O_2$ in 50 mM MOPS, pH 8.0, then the reaction was stopped with
321 the addition of 0.071 $U.\mu l^{-1}$ of catalase followed by desalting. PcuC Cu-loading was performed by
322 incubating the protein (200 µM) with 2 to 10 equiv. of $CuSO_4$ in MOPS 50 mM followed by desalting. For
323 Cu-loading before oxaziridine labeling, 5 equiv. of $CuSO_4$ were used. Oxaziridine labeling was made by
324 incubating PcuC (14 or 100 µM) with 0, 0.1, 0.5, 1, 5 or 10 equiv. of the probe for 20 or 30 min in 50 mM
325 MOPS, pH 8.0 followed by desalting. For in-gel fluorescence analysis, oxaziridine-labeled PcuC was
326 incubated with 10 equiv. of DBCO-Cy5 overnight in 50 mM MOPS, pH 8.0 and excess reagent was removed
327 by ultrafiltration (5 kDa cutoff, Vivaspin 500, Sartorius).

328 **4.3. Mass spectrometry analyses**

329 ESI-MS analyses were performed as described [20]. For proteolysis and LC-MS/MS analyses, 20 µL of
330 PcuC solution (7 µM) in 50 mM MOPS buffer (pH 8.0) with 20% acetonitrile (ACN) were digested by
331 adding 3 µL of trypsin/Lys C (Promega) at a concentration of 12.5 $ng.\mu L^{-1}$ in 0.1% formic acid (FA) for 3 h
332 at 37°C. For TMT labeling, the manufacturer's protocol (ThermoFisher) was followed. Peptides from each
333 experimental condition (various concentrations of oxaziridine or different reaction times with $H_2{}^{18}O_2$) were
334 incubated with one of the six 6-plex TMT reagents, consisting of reporter ions 126, 127, 128, 129, 130, and
335 131 (0.8 mg in 41 µL of anhydrous ACN) for 1 h at room temperature. The reactions were quenched by
336 adding 2 µL of 5% ammonium hydroxide for 15 minutes. For each experiment (oxaziridine or $H_2{}^{18}O_2$), the
337 six conditions were pooled and diluted in 300 µL of 0.1% trifluoroacetic acid (TFA). The labeled peptides
338 were filtered using a C18 column (ThermoFisher) to remove excess TMT reagents, eluted with 2×300 µL
339 of 50% ACN/0.1% TFA, and dried using a SpeedVac. The dried samples were reconstituted in 2%
340 ACN/0.1% FA to achieve a theoretical protein concentration of 1 $\mu g.\mu L^{-1}$. The samples were injected into
341 an LC-MS/MS system using a high-performance nano-liquid chromatography (UHPLC RSLC,
342 ThermoFisher) equipped with online desalting (PEPMAP C18, 5 µm, 300 Å trap column, 300 µm × 5 mm),
343 coupled to a Q-Exactive Plus hybrid mass spectrometer (ThermoFisher). The analytical column used was
344 an Acclaim PepMap RSLC capillary column (nanoViper C18, 2 µm, 100 Å, 75 µm × 15 cm). The gradient
345 for peptide elution was as follows: solvent A: 0.1% FA, solvent B: ACN with 0.1% FA. The gradient
346 program included the following steps: (1) 2.5–25% B over 57 min, (2) 25–50% B over 6 min, (3) 50–90%
347 B in 1 min, and (4) 90% B for 10 min. A data-dependent acquisition (DDA) method was employed with a
348 Top10 approach, where the 10 most abundant peptides were selected for fragmentation in each survey scan.
349 MS settings were: precursor mass range 375 to 1400 m/z, resolution 70,000, AGC target $3\times10^6$, maximum
350 IT 100 ms. MS/MS parameters: fragment mass range 100 to 2000 m/z, resolution 70,000, AGC target $2\times10^5$,
351 and normalized collision energy of 27 (33 for TMT-labeled samples). Peak list files in .mgf format (Mascot
352 Generic Format) were generated using Proteome Discoverer 2.4 (ThermoFisher). Protein identification was
353 carried out using MASCOT 2.3 software, querying a database containing PcuC and common contaminants

354 (246 sequences, including trypsin, keratins, etc.). Search parameters were set as follows: trypsin as the
355 digestion enzyme, up to 4 missed cleavages, precursor mass tolerance of 10 ppm, product ion mass accuracy
356 of 0.02 Da, with fixed modifications of TMT6plex (N-term) and TMT6plex (K), and variable modifications
357 including deamidation (Gln, Asn), $^{16}$O-oxidation (Met, monoisotopic mass = 15.994915 Da), $^{18}$O-oxidation
358 (Met, monoisotopic mass = 17.99916), $^{16}$O-dioxidation (Met, monoisotopic mass = 31.989829 Da), $^{18}$O-
359 dioxidation (Met, monoisotopic mass = 35.998321 Da), $^{16}$O/$^{18}$O-dioxidation (Met, monoisotopic mass =
360 33.994075 Da) or oxaziridine modification (Met, monoisotopic mass = 167.080710 Da). Quantification was
361 performed by exporting reporter ion intensity data for all peptides to Excel using Mascot software. The
362 percentages were determined by summing, for each Met, the relative intensities of all detected forms. For
363 the $H_2{}^{18}O_2$ treatment, $^{18}$O-containing oxidation states ($^{18}$O-sulfoxide, $^{18}$O-sulfone, and $^{16}$O/$^{18}$O-sulfone) were
364 grouped as oxidized Met, while non-modified and $^{16}$O-oxidized forms, considered artifactual, were counted
365 as non-oxidized. Note that, according to the manufacturer, the $^{18}$O-labeled hydrogen peroxide solution may
366 contain up to 10% of $H_2{}^{16}O_2$ but because the exact value was not determined, this parameter was not
367 considered for calculation. Similarly, for the oxaziridine treatment, non-modified and $^{16}$O-oxidized forms
368 were considered as non-labeled.

369 **4.4. PcuC crystallization and structure analysis**

370 Crystals of PcuC were obtained by the sitting drop method using 96 wells plates and a pipetting robot
371 (TECAN Evoware). The apo protein was concentrated to 26 mg.mL$^{-1}$ and crystals were obtained by mixing
372 1 µL of protein with 1 µL of 1.2 M sodium citrate and 0.1 M Tris pH 8.5. Crystals quickly appeared and,
373 after supplementing the mother liquor with 15% glycerol, a few crystals were flash frozen directly in liquid
374 nitrogen. Crystals were collected at the SOLEIL synchrotron (France) and the structure of apo PcuC was
375 then solved at 1.05 Å resolution in a $P4_32_12$ space group. To obtain experimental data on copper binding to
376 PcuC, ten copper equivalents were added to the protein and crystallization of the protein was rescreened.
377 Crystals were obtained in a condition containing 25% PEG 3350 and 20 mM $CaCl_2$, 20 mM $CdCl_2$ and 20
378 mM $CoCl_2$. This crystal form diffracted to 2.1 Å resolution, however it is affected by a translational NCS

379 (tNCS) that, together with the three molecules in the asymmetric unit, appeared to be difficult to refine ($R$
380 = 30.2%; $R_{free}$ = 36.5%). This structure is therefore not presented, although it clearly showed three sites of
381 high electron density, all of them relatively close to each other. Data collection at different wavelengths
382 (copper and cobalt edges) also indicated that one site was occupied by copper, whereas the two others were
383 cadmium ions. Additional screens were used to find a different crystal form that would not grow in a
384 complex mixture of metal and that would eventually not be affected by tNCS. A crystal form was obtained
385 in a condition containing 20% PEG 6000, 1 M $LiCl_2$ and 0.1 M citric acid at pH 4.0. It diffracted to 2.75Å
386 resolution and was refined to a $R$ and $R_{free}$ of 24.2% and 30.4%, respectively.

387 Prediction of intrinsically disordered region was made using IUpred2A [51]. Solvent exposure of Met
388 was determined using the "*get_area*" function with default parameters and partial charges were determined
389 using APBS Electrostatics plugin of PyMol 3.1.0a0 (open-source build).

## Supplementary data

Supplemental Results, Supplemental Discussion, Fig. S1-S8, Table S1, Supplemental References.

## Data availability

The mass spectrometry proteomics data have been deposited to the ProteomeXchange Consortium via the PRIDE [52,53] partner repository with the dataset identifier PXD062219.

## Declaration of Competing Interest

The authors declare that they have no known competing financial interests or personal relationships that could have appeared to influence the work reported in this paper.


## Acknowledgments

The authors kindly thank the support team of Aix Marseille Univ., INRAE, Biodiversité et Biotechnologies Fongiques – Chantal Parodi-Negri, Naura Thibeau and Christophe Boyer. This research was funded by the Commissariat à l'Energie Atomique et aux Energies Alternatives (CEA) and by the project METOXIC [ANR 16-CE11-0012]. This work received support from the French government under the France 2030 investment plan, as part of the Initiative d'Excellence d'Aix-Marseille Université —IM2B (AMX-19-IET-006) for L.M. and L.T. – A*MIDEX (AMX-21-PEP-028) for L.T, and from the NovoNordisk foundation (OxyMiST project, grant number NNF20OC0059697).


## CRediT author statement

**Lionel Tarrago:** Conceptualization, Methodology, Validation, Formal analysis, Investigation, Resources, Data Curation, Writing - Original Draft, Writing - Review & Editing, Visualization, Supervision, Funding acquisition, Project administration. **Lise Molinelli:** Conceptualization, Methodology, Validation, Formal analysis, Investigation, Data Curation, Writing - Review & Editing. **Maya Belghazi:** Conceptualization, Methodology, Validation, Formal analysis, Investigation, Data Curation, Writing - Review & Editing. **Mathilde Tribout:** Formal analysis, Investigation, Data Curation. **David Lemaire:** Methodology,

Validation, Formal analysis, Investigation, Data Curation. **Pierre Legrand:** Methodology, Validation, Formal analysis, Investigation, Data Curation. **Sandrine Grosse:** Formal analysis, Investigation, Data Curation. **David Pignol**: Conceptualization, Methodology, Supervision, Funding acquisition, Writing - Review & Editing. **Monique Sabaty:** Conceptualization, Methodology, Supervision, Funding acquisition, Writing - Review & Editing. **Thierry Tron:** Conceptualization, Methodology, Supervision, Funding acquisition, Writing - Review & Editing. **Pascal Arnoux:** Conceptualization, Methodology, Validation, Formal analysis, Investigation, Resources, Data Curation, Writing - Original Draft, Writing - Review & Editing, Visualization, Supervision, Funding acquisition, Project administration.

**Declaration of generative AI in scientific writing**

During the preparation of this work the authors used ChatGPT to improve the clarity and readability of the text. After using this tool, the author reviewed and edited the content as needed and take full responsibility for the content of the publication

## References


[1] F.W. Outten, B.S. Twining, Metal Homeostasis, in: Wiley Encyclopedia of Chemical Biology, John Wiley & Sons, Ltd, 2008: pp. 1–10. https://doi.org/10.1002/9780470048672.wecb324.

[2] J.T. Rubino, K.J. Franz, Coordination chemistry of copper proteins: How nature handles a toxic cargo for essential function, Journal of Inorganic Biochemistry 107 (2012) 129–143. https://doi.org/10.1016/j.jinorgbio.2011.11.024.

[3] R.M. Rasia, C.W. Bertoncini, D. Marsh, W. Hoyer, D. Cherny, M. Zweckstetter, C. Griesinger, T.M. Jovin, C.O. Fernández, Structural characterization of copper(II) binding to α-synuclein: Insights into the bioinorganic chemistry of Parkinson's disease, Proc Natl Acad Sci U S A 102 (2005) 4294–4299. https://doi.org/10.1073/pnas.0407881102.

[4] J.H. Viles, F.E. Cohen, S.B. Prusiner, D.B. Goodin, P.E. Wright, H.J. Dyson, Copper binding to the prion protein: Structural implications of four identical cooperative binding sites, Proceedings of the National Academy of Sciences 96 (1999) 2042–2047. https://doi.org/10.1073/pnas.96.5.2042.

[5] J. Arguello, D. Raimunda, T. Padilla-Benavides, Mechanisms of copper homeostasis in bacteria, Frontiers in Cellular and Infection Microbiology 3 (2013). https://www.frontiersin.org/article/10.3389/fcimb.2013.00073 (accessed May 9, 2022).

[6] J.A. Imlay, Where in the world do bacteria experience oxidative stress?, Environ. Microbiol. 21 (2019) 521–530. https://doi.org/10.1111/1462-2920.14445.

[7] C.L. Hawkins, M.J. Davies, Detection, identification, and quantification of oxidative protein modifications, J. Biol. Chem. 294 (2019) 19683–19708. https://doi.org/10.1074/jbc.REV119.006217.

[8] M.J. Davies, The oxidative environment and protein damage, Biochim. Biophys. Acta 1703 (2005) 93–109. https://doi.org/10.1016/j.bbapap.2004.08.007.

[9] M.K. Tiwari, P.M. Hägglund, I.M. Møller, M.J. Davies, M.J. Bjerrum, Copper ion / H2O2 oxidation of Cu/Zn-Superoxide dismutase: Implications for enzymatic activity and antioxidant action, Redox Biol 26 (2019) 101262. https://doi.org/10.1016/j.redox.2019.101262.

[10] B. Bissaro, Å.K. Røhr, G. Müller, P. Chylenski, M. Skaugen, Z. Forsberg, S.J. Horn, G. Vaaje-Kolstad, V.G.H. Eijsink, Oxidative cleavage of polysaccharides by monocopper enzymes depends on H2O2, Nat. Chem. Biol. 13 (2017) 1123–1128. https://doi.org/10.1038/nchembio.2470.

[11] D. Kracher, M. Andlar, P.G. Furtmüller, R. Ludwig, Active-site copper reduction promotes substrate binding of fungal lytic polysaccharide monooxygenase and reduces stability, Journal of Biological Chemistry 293 (2018) 1676–1687. https://doi.org/10.1074/jbc.RA117.000109.

[12] A. Paradisi, E.M. Johnston, M. Tovborg, C.R. Nicoll, L. Ciano, A. Dowle, J. McMaster, Y. Hancock, G.J. Davies, P.H. Walton, Formation of a Copper(II)–Tyrosyl Complex at the Active Site of Lytic Polysaccharide Monooxygenases Following Oxidation by H2O2, J. Am. Chem. Soc. 141 (2019) 18585–18599. https://doi.org/10.1021/jacs.9b09833.

[13] E. Ponzini, A. De Palma, L. Cerboni, A. Natalello, R. Rossi, R. Moons, A. Konijnenberg, J. Narkiewicz, G. Legname, F. Sobott, P. Mauri, C. Santambrogio, R. Grandori, Methionine oxidation in α-synuclein inhibits its propensity for ordered secondary structure, J Biol Chem 294 (2019) 5657–5665. https://doi.org/10.1074/jbc.RA118.001907.

[14] N.D. Younan, R.C. Nadal, P. Davies, D.R. Brown, J.H. Viles, Methionine oxidation perturbs the structural core of the prion protein and suggests a generic misfolding pathway, J Biol Chem 287 (2012) 28263–28275. https://doi.org/10.1074/jbc.M112.354779.

[15] J.T. Rubino, P. Riggs-Gelasco, K.J. Franz, Methionine motifs of copper transport proteins provide general and flexible thioether-only binding sites for Cu(I) and Ag(I), J. Biol. Inorg. Chem. 15 (2010) 1033–1049. https://doi.org/10.1007/s00775-010-0663-9.

471 [16] J.T. Rubino, M.P. Chenkin, M. Keller, P. Riggs-Gelasco, K.J. Franz, A comparison of methionine,
472 histidine and cysteine in copper(i)-binding peptides reveals differences relevant to copper uptake
473 by organisms in diverse environments, Metallomics 3 (2011) 61–73.
474 https://doi.org/10.1039/c0mt00044b.
475 [17] U. Contaldo, D. Savant-Aira, A. Vergnes, J. Becam, F. Biaso, M. Ilbert, L. Aussel, B. Ezraty, E. Lojou, I.
476 Mazurenko, Methionine-rich domains emerge as facilitators of copper recruitment in detoxification
477 systems, Proceedings of the National Academy of Sciences 121 (2024) e2402862121.
478 https://doi.org/10.1073/pnas.2402862121.
479 [18] L. Macomber, C. Rensing, J.A. Imlay, Intracellular copper does not catalyze the formation of
480 oxidative DNA damage in Escherichia coli, J Bacteriol 189 (2007) 1616–1626.
481 https://doi.org/10.1128/JB.01357-06.
482 [19] A. Gennaris, B. Ezraty, C. Henry, R. Agrebi, A. Vergnes, E. Oheix, J. Bos, P. Leverrier, L. Espinosa, J.
483 Szewczyk, D. Vertommen, O. Iranzo, J.-F. Collet, F. Barras, Repairing oxidized proteins in the
484 bacterial envelope using respiratory chain electrons, Nature 528 (2015) 409–412.
485 https://doi.org/10.1038/nature15764.
486 [20] L. Tarrago, S. Grosse, M.I. Siponen, D. Lemaire, B. Alonso, G. Miotello, J. Armengaud, P. Arnoux, D.
487 Pignol, M. Sabaty, Rhodobactersphaeroides methionine sulfoxide reductase P reduces R- and S-
488 diastereomers of methionine sulfoxide from a broad-spectrum of protein substrates, Biochem. J.
489 475 (2018) 3779–3795. https://doi.org/10.1042/BCJ20180706.
490 [21] A. Vergnes, C. Henry, G. Grassini, L. Loiseau, S. El Hajj, Y. Denis, A. Galinier, D. Vertommen, L.
491 Aussel, B. Ezraty, Periplasmic oxidized-protein repair during copper stress in E. coli: A focus on the
492 metallochaperone CusF, PLoS Genet 18 (2022) e1010180.
493 https://doi.org/10.1371/journal.pgen.1010180.
494 [22] F.L. Sousa, R.J. Alves, M.A. Ribeiro, J.B. Pereira-Leal, M. Teixeira, M.M. Pereira, The superfamily of
495 heme-copper oxygen reductases: types and evolutionary considerations, Biochim Biophys Acta
496 1817 (2012) 629–637. https://doi.org/10.1016/j.bbabio.2011.09.020.
497 [23] L.A. Abriata, L. Banci, I. Bertini, S. Ciofi-Baffoni, P. Gkazonis, G.A. Spyroulias, A.J. Vila, S. Wang,
498 Mechanism of Cu(A) assembly, Nat. Chem. Biol. 4 (2008) 599–601.
499 https://doi.org/10.1038/nchembio.110.
500 [24] F. Canonica, D. Klose, R. Ledermann, M.M. Sauer, H.K. Abicht, N. Quade, A.D. Gossert, S. Chesnov,
501 H.-M. Fischer, G. Jeschke, H. Hennecke, R. Glockshuber, Structural basis and mechanism for
502 metallochaperone-assisted assembly of the CuA center in cytochrome oxidase, Sci Adv 5 (2019)
503 eaaw8478. https://doi.org/10.1126/sciadv.aaw8478.
504 [25] L. Hederstedt, Diversity of Cytochrome c Oxidase Assembly Proteins in Bacteria, Microorganisms 10
505 (2022) 926. https://doi.org/10.3390/microorganisms10050926.
506 [26] A.K. Thompson, J. Gray, A. Liu, J.P. Hosler, The roles of Rhodobacter sphaeroides copper
507 chaperones PCu(A)C and Sco (PrrC) in the assembly of the copper centers of the aa(3)-type and the
508 cbb(3)-type cytochrome c oxidases, Biochim. Biophys. Acta 1817 (2012) 955–964.
509 https://doi.org/10.1016/j.bbabio.2012.01.003.
510 [27] A.K. Boal, A.C. Rosenzweig, Structural Biology of Copper Trafficking, Chem. Rev. 109 (2009) 4760–
511 4779. https://doi.org/10.1021/cr900104z.
512 [28] R.A. Festa, D.J. Thiele, Copper: An essential metal in biology, Current Biology 21 (2011) R877–R883.
513 https://doi.org/10.1016/j.cub.2011.09.040.
514 [29] S. Iwata, C. Ostermeier, B. Ludwig, H. Michel, Structure at 2.8 A resolution of cytochrome c oxidase
515 from Paracoccus denitrificans, Nature 376 (1995) 660–669. https://doi.org/10.1038/376660a0.
516 [30] H.K. Abicht, M.A. Schärer, N. Quade, R. Ledermann, E. Mohorko, G. Capitani, H. Hennecke, R.
517 Glockshuber, How periplasmic thioredoxin TlpA reduces bacterial copper chaperone ScoI and

518 cytochrome oxidase subunit II (CoxB) prior to metallation, J Biol Chem 289 (2014) 32431–32444.
519 https://doi.org/10.1074/jbc.M114.607127.
520 [31] L. Banci, I. Bertini, S. Ciofi-Baffoni, E. Katsari, N. Katsaros, K. Kubicek, S. Mangani, A copper(I)
521 protein possibly involved in the assembly of CuA center of bacterial cytochrome c oxidase, Proc.
522 Natl. Acad. Sci. U.S.A. 102 (2005) 3994–3999. https://doi.org/10.1073/pnas.0406150102.
523 [32] O.S. Fisher, M.R. Sendzik, M.O. Ross, T.J. Lawton, B.M. Hoffman, A.C. Rosenzweig, PCuAC domains
524 from methane-oxidizing bacteria use a histidine brace to bind copper, J. Biol. Chem. 294 (2019)
525 16351–16363. https://doi.org/10.1074/jbc.RA119.010093.
526 [33] H. Liu, G. Ponniah, A. Neill, R. Patel, B. Andrien, Accurate Determination of Protein Methionine
527 Oxidation by Stable Isotope Labeling and LC-MS Analysis, Anal. Chem. 85 (2013) 11705–11709.
528 https://doi.org/10.1021/ac403072w.
529 [34] J.Q. Bettinger, K.A. Welle, J.R. Hryhorenko, S. Ghaemmaghami, Quantitative Analysis of in Vivo
530 Methionine Oxidation of the Human Proteome, J Proteome Res 19 (2020) 624–633.
531 https://doi.org/10.1021/acs.jproteome.9b00505.
532 [35] L. Molinelli, E. Drula, J.-C. Gaillard, D. Navarro, J. Armengaud, J.-G. Berrin, T. Tron, L. Tarrago,
533 Methionine oxidation of carbohydrate-active enzymes during white-rot wood decay, Appl Environ
534 Microbiol 90 (2024) e0193123. https://doi.org/10.1128/aem.01931-23.
535 [36] S. Lin, X. Yang, S. Jia, A.M. Weeks, M. Hornsby, P.S. Lee, R.V. Nichiporuk, A.T. Iavarone, J.A. Wells,
536 F.D. Toste, C.J. Chang, Redox-based reagents for chemoselective methionine bioconjugation,
537 Science 355 (2017) 597–602. https://doi.org/10.1126/science.aal3316.
538 [37] S.K. Elledge, H.L. Tran, A.H. Christian, V. Steri, B. Hann, F.D. Toste, C.J. Chang, J.A. Wells, Systematic
539 identification of engineered methionines and oxaziridines for efficient, stable, and site-specific
540 antibody bioconjugation, Proc. Natl. Acad. Sci. U.S.A. (2020).
541 https://doi.org/10.1073/pnas.1920561117.
542 [38] E. Weerapana, C. Wang, G.M. Simon, F. Richter, S. Khare, M.B.D. Dillon, D.A. Bachovchin, K.
543 Mowen, D. Baker, B.F. Cravatt, Quantitative reactivity profiling predicts functional cysteines in
544 proteomes, Nature 468 (2010) 790–795. https://doi.org/10.1038/nature09472.
545 [39] D. He, H. Feng, B. Sundberg, J. Yang, J. Powers, A.H. Christian, J.E. Wilkinson, C. Monnin, D.
546 Avizonis, C.J. Thomas, R.A. Friedman, M.D. Kluger, M.A. Hollingsworth, P.M. Grandgenett, K.A.
547 Klute, F.D. Toste, C.J. Chang, I.I.C. Chio, Methionine oxidation activates pyruvate kinase M2 to
548 promote pancreatic cancer metastasis, Mol Cell 82 (2022) 3045-3060.e11.
549 https://doi.org/10.1016/j.molcel.2022.06.005.
550 [40] C.-C. Chao, Y.-S. Ma, E.R. Stadtman, Modification of protein surface hydrophobicity and methionine
551 oxidation by oxidative systems, Proceedings of the National Academy of Sciences 94 (1997) 2969–
552 2974. https://doi.org/10.1073/pnas.94.7.2969.
553 [41] L. Tarrago, A. Kaya, E. Weerapana, S.M. Marino, V.N. Gladyshev, Methionine sulfoxide reductases
554 preferentially reduce unfolded oxidized proteins and protect cells from oxidative protein unfolding,
555 J. Biol. Chem. 287 (2012) 24448–24459. https://doi.org/10.1074/jbc.M112.374520.
556 [42] K.L.I.M. Blundell, M.A. Hough, E. Vijgenboom, J.A.R. Worrall, Structural and mechanistic insights
557 into an extracytoplasmic copper trafficking pathway in Streptomyces lividans, Biochemical Journal
558 459 (2014) 525–538. https://doi.org/10.1042/BJ20140017.
559 [43] E.J. Walker, J.Q. Bettinger, K.A. Welle, J.R. Hryhorenko, A.M. Molina Vargas, M.R. O'Connell, S.
560 Ghaemmaghami, Protein folding stabilities are a major determinant of oxidation rates for buried
561 methionine residues, Journal of Biological Chemistry (2022) 101872.
562 https://doi.org/10.1016/j.jbc.2022.101872.
563 [44] I. Dalle-Donne, R. Rossi, D. Giustarini, N. Gagliano, P. Di Simplicio, R. Colombo, A. Milzani,
564 Methionine oxidation as a major cause of the functional impairment of oxidized actin, Free Radical
565 Biology and Medicine 32 (2002) 927–937. https://doi.org/10.1016/S0891-5849(02)00799-2.

[45] H. Pan, K. Chen, L. Chu, F. Kinderman, I. Apostol, G. Huang, Methionine oxidation in human IgG2 Fc decreases binding affinities to protein A and FcRn, Protein Science 18 (2009) 424–433. https://doi.org/10.1002/pro.45.

[46] E. Vandermarliere, B. Ghesquière, V. Jonckheere, K. Gevaert, L. Martens, Unraveling the specificities of the different human methionine sulfoxide reductases, Proteomics 14 (2014) 1990–1998. https://doi.org/10.1002/pmic.201300357.

[47] J.Q. Bettinger, M. Simon, A. Korotkov, K.A. Welle, J.R. Hryhorenko, A. Seluanov, V. Gorbunova, S. Ghaemmaghami, Accurate Proteomewide Measurement of Methionine Oxidation in Aging Mouse Brains, J Proteome Res 21 (2022) 1495–1509. https://doi.org/10.1021/acs.jproteome.2c00127.

[48] S. Kar, S. Sen, S. Maji, D. Saraf, Ruturaj, R. Paul, S. Dutt, B. Mondal, E. Rodriguez-Boulan, R. Schreiner, D. Sengupta, A. Gupta, Copper(II) import and reduction are dependent on His-Met clusters in the extracellular amino terminus of human copper transporter-1, Journal of Biological Chemistry 298 (2022). https://doi.org/10.1016/j.jbc.2022.101631.

[49] L. Tarrago, S. Grosse, D. Lemaire, L. Faure, M. Tribout, M.I. Siponen, M. Kojadinovic-Sirinelli, D. Pignol, P. Arnoux, M. Sabaty, Reduction of Protein Bound Methionine Sulfoxide by a Periplasmic Dimethyl Sulfoxide Reductase, Antioxidants 9 (2020) 616. https://doi.org/10.3390/antiox9070616.

[50] S.P. Wolff, [18] Ferrous ion oxidation in presence of ferric ion indicator xylenol orange for measurement of hydroperoxides, in: Methods in Enzymology, Academic Press, 1994: pp. 182–189. https://doi.org/10.1016/S0076-6879(94)33021-2.

[51] B. Mészáros, G. Erdős, Z. Dosztányi, IUPred2A: context-dependent prediction of protein disorder as a function of redox state and protein binding, Nucleic Acids Research 46 (2018) W329–W337. https://doi.org/10.1093/nar/gky384.

[52] Y. Perez-Riverol, C. Bandla, D.J. Kundu, S. Kamatchinathan, J. Bai, S. Hewapathirana, N.S. John, A. Prakash, M. Walzer, S. Wang, J.A. Vizcaíno, The PRIDE database at 20 years: 2025 update, Nucleic Acids Res 53 (2025) D543–D553. https://doi.org/10.1093/nar/gkae1011.

[53] E.W. Deutsch, N. Bandeira, Y. Perez-Riverol, V. Sharma, J.J. Carver, L. Mendoza, D.J. Kundu, S. Wang, C. Bandla, S. Kamatchinathan, S. Hewapathirana, B.S. Pullman, J. Wertz, Z. Sun, S. Kawano, S. Okuda, Y. Watanabe, B. MacLean, M.J. MacCoss, Y. Zhu, Y. Ishihama, J.A. Vizcaíno, The ProteomeXchange consortium at 10 years: 2023 update, Nucleic Acids Res 51 (2023) D1539–D1548. https://doi.org/10.1093/nar/gkac1040.